Newer Non-ionic A_2B_2-Type Enzyme-Responsive Amphiphiles for Drug Delivery

Krishna,[a] Badri Parshad,[a, b] Katharina Achazi,[c] Christoph Böttcher,[d] Rainer Haag,[c] and Sunil K. Sharma*[a]

A new series of nonionic gemini amphiphiles have been synthesized in a multi-step chemoenzymatic approach by using a novel A_2B_2-type central core consisting of conjugating glycerol and propargyl bromide on 5-hydroxy isophthalic acid. A pair of hydrophilic monomethoxy poly(ethylene glycol) (mPEG) and hydrophobic linear alkyl chains (C_{12}/C_{15}) were then added to the core to obtain amphiphilic architectures. The aggregation tendency in aqueous media was studied by dynamic light scattering, fluorescence spectroscopy and cryogenic transmission electron microscopy. The nanotransport potential of the amphiphiles was studied for model hydrophobic guests, that is, the dye Nile Red and the drug Nimodipine by using UV/Vis and fluorescence spectroscopy. Evaluation of the viability of amphiphile-treated A549 cells showed them to be well tolerated up to the concentrations studied. Being ester based, these amphiphiles exhibit stimuli-responsive sensitivity towards esterases, and a rupture of amphiphilic architecture was observed in the presence of immobilized *Candida antarctica* lipase (Novozym 435), thus facilitating release of the encapsulated guest from the aggregate.

Introduction

Self-assembly and self-organization are the key tools in supramolecular chemistry and are being intensively used by researchers to build amazingly complex architectures.[1] The advent of supramolecular chemistry in the last decades of the 20th century has provided chemists with a wealth of new routes toward constructing molecular structures and materials that exhibit self-assembly phenomenon due to relatively weak, non-covalent interactions, such as hydrogen bonding, π-π stacking, electrostatic and van der Waals interactions.[1,2] Such assemblies are usually stabilized by thermodynamics (relative free energies, enthalpy and entropy of binding) and/or kinetic aspect,[3] and provide several hierarchical levels of molecular organization. The self-assembly of amphiphiles has been shown to be of significant importance in many research fields, such as building blocks for the fabrication of novel organic nanofibers or nanotubes for electrical and medical devices,[4–6] candidates for drug delivery,[7,8] nano-/microreactors for carrying out reactions in aqueous solution, artificial enzyme-mimicking,[9,10] stabilizers for emulsions used for cleaning and green organic reactions.[11,12] Moreover, amphiphiles show unique and newer opportunities for designing novel material for advanced applications in biomedicine and bio-nanotechnology.[13–15] The hydrophilic and hydrophobic groups of amphiphiles enable them to self-assemble at an interface or in solution to form diverse molecular assemblies. The size and morphology of these assemblies such as micelles, toroids, monolayers, vesicles, rods and sheet-like structures are dictated by the nature of substituents and hydrophilic-lipophilic balance (HLB).[16–20] The self-assembly is accompanied by the creation of a hydrophobic space surrounded by hydrophilic groups and this arrangement provides an attractive opportunity to address the challenges of drug delivery, such as insufficient aqueous solubility of drug, shorter half-life in the bloodstream, lack of selectivity, and high overall clearance rate. Nanocarriers are known to provide the drug a protective lipophilic environment, enhance the circulation period in blood, and facilitate active site targeting, and thus minimizing drug degradation and loss upon administration, and prevent harmful or undesired side-effects.[21–24]

Amphiphiles can be broadly divided into two major classes each having its own advantages, although, polymeric amphiphiles form relatively stable nanostructures, small molecule amphiphiles (SMAs) on the other hand are easy to design and their self-assemblies display more similarity with the natural analogs.[25–30] Furthermore, small amphiphilic systems can be either ionic or nonionic whereas, ionic, particularly cationic systems are known to be cytotoxic to varying extent.[31–33]

Among SMAs, gemini and dimeric amphiphiles, characterized by the presence of two hydrophilic head groups and two hydrophobic tails, linked by a rigid or flexible spacer, received considerable attention, due to their unique properties such as self-assembly behavior,[34,35] enhanced micellar stability,[36–38] high wetting ability, multiple aggregate morphologies, low

[a] *Krishna, Dr. B. Parshad, Prof. S. K. Sharma*
Department of Chemistry, University of Delhi
Delhi, 110007 (India)
E-mail: sksharma@chemistry.du.ac.in
[b] *Dr. B. Parshad*
Department of Chemical Engineering and Biotechnology
University of Cambridge
Cambridge, CB3 0AS (UK)
[c] *Dr. K. Achazi, Prof. Dr. R. Haag*
Institut für Chemie und Biochemie
Freie Universität Berlin
Takustraße 3, 14195 Berlin (Germany)
[d] *Dr. C. Böttcher*
Forschungszentrum für Elektronenmikroskopie
Institut für Chemie und Biochemie
Freie Universität Berlin
Fabeckstraße 36a, 14195 Berlin (Germany)

Supporting information for this article is available on the WWW under https://doi.org/10.1002/cmdc.202100031

Krafft temperature and excellent lime-soap dispersing properties as compared with the monomeric single-chain amphiphilic analogues.[39–42] The above factors bring focus on gemini amphiphiles for use in biomedical applications. Our interest is to explore the drug delivery potential of newer types of amphiphiles. Considering various possible structures among gemini amphiphiles, the nonionic one is advantageous for the drug delivery applications due to reduced cytotoxicity.[43–45] Furthermore, the presence of two hydrophobic alkyl tails in gemini amphiphiles allow sharp and uniform decrease in CAC value than their monomeric counterparts and thus making a valuable contribution for therapeutic applications. Nonionic gemini amphiphiles based on carbohydrates are known in the literature.[46,47] As a part of our ongoing efforts to explore the use of other type of competing novel moieties,[3,48–52] we aim to explore the use of gold-standard poly(ethylene glycol) (PEG) towards the synthesis of a wide variety of amphiphiles for drug delivery applications, PEG is known for its unique properties, such as low toxicity, excellent solubility in aqueous solution, good chemical stability, ion-transporting ability, decreased interaction with blood components, etc.[23,53,54] PEGylation is an established method for increasing protein stability or solubilizing hydrophobic biomolecules as well as reduce immunogenicity and antigenicity. PEG's hydrophilic surface allows prolonged circulation of polymeric micelles in the bloodstream.[55–57] The other building block, that is, 5-hydroxyisophthalate was considered on the basis that its PEG based block copolymer reported earlier by Kumar et al. is nontoxic and highly efficient drug delivery vehicles for hydrophobic and partially hydrophilic drugs.[58] The synthesis of stimuli responsive delivery systems is another desirable feature for controlled drug delivery. Our interest is to develop enzyme responsive drug delivery system (DDS). Cells contain a variety of enzymes, such as esterase, Camacho, lipase, phospholipase and nuclease, etc., but in the tumor tissues some specific enzymes, such as matrix metalloproteinase, phospholipase, esterase are present in higher amount than the other normal tissues. Esterase-responsive nanoparticles could thus be sensitive for tumor cells due to the overexpressed esterase in tumor cells. Esterase-responsive micellar nanoparticle is thus considered as one of the best strategies for drug delivery.[59]

Herein, we report the design, synthesis, and characterization of a newer family of glycerol based nonionic gemini amphiphiles and study of their supramolecular aggregation into different nanostructures in an aqueous medium. Firstly, suitably protected glycerol was conjugated via its secondary hydroxy group with the 5-hydroxy isophthalic acid via Mitsunobu reaction and the resulting diacid then undergoes esterification with propargyl alcohol to yield an A_2B_2 central core in a multiple step chemoenzymatic approach by making use of immobilized *C. antarctica* lipase (Novozym 435). The primary alcohols of the glyceryl moiety in the A_2B_2 core were first reacted with the long-chain aliphatic acid, it was followed by the reaction of mPEG-azide to couple with the two acetylenic groups of the core by click coupling (Figure 1). The amphiphiles thus generated by conferring hydrophobic and hydrophilic groups were studied for their transport potential.

Results and Discussion

The gemini amphiphiles were synthesized by following the Novozym 435 catalyzed chemoenzymatic approach and their supramolecular organization were characterized physicochemically by using infrared spectroscopy (IR), elemental analysis, gel permeation chromatography (GPC), dynamic light scattering (DLS), cryogenic transmission electron microscopy (*cryo*-TEM), high-resolution transmission electron microscopy (HRTEM), critical aggregation concentration (CAC) and ^{1}H, ^{13}C NMR spectroscopy. Nile Red and Nimodipine were used as a model dye/drug in order to explore the solubilization tendency of the amphiphiles.

Synthesis and characterization

A_2B_2 type central core (**7**) of gemini amphiphiles were synthesized from commercially available glycerol (**1**) and dimethyl 5-hydroxyisophthalate (**3**) following the strategy as outlined in Scheme 1.

Glycerol (**1**) was first converted to 2-hydroxypropane-1,3-diyl diacetate (**2**) using vinyl acetate and Novozym 435 as a

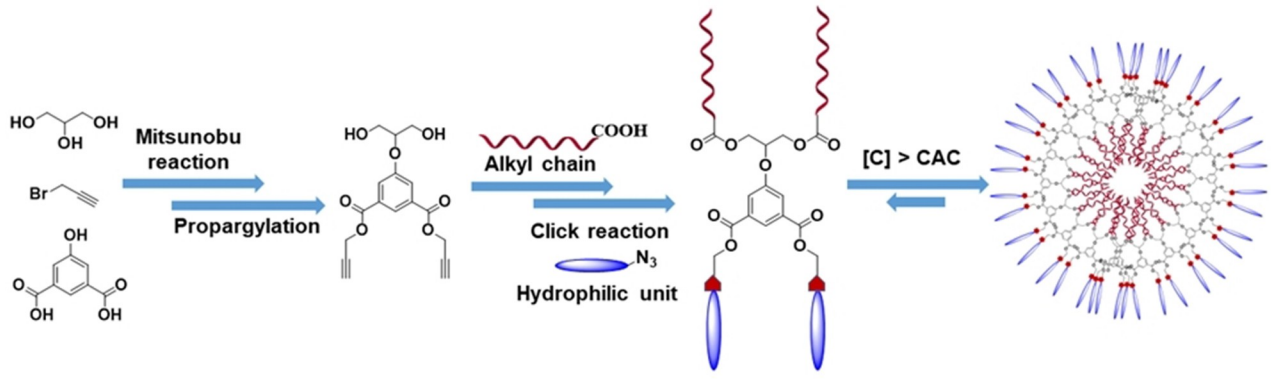

Figure 1. Representation of the synthetic approach and self-assembly of the amphiphiles in aqueous media.

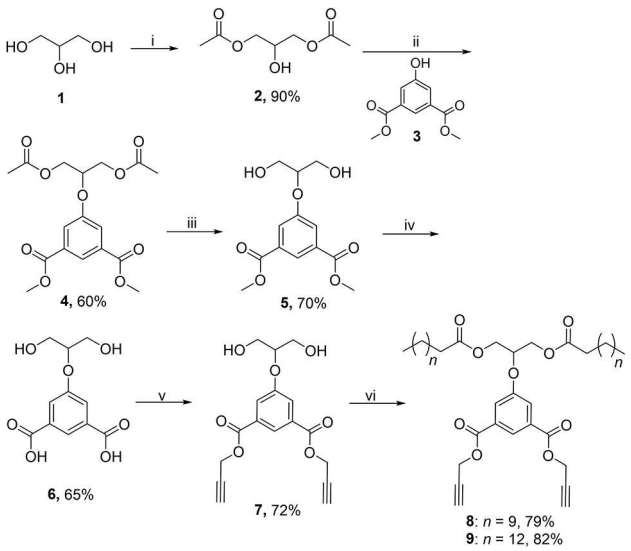

Scheme 1. Synthesis of the A_2B_2 core and its functionalization with hydrophobic moieties. i) vinyl acetate, Novozym 435, THF, 40 °C, 3 h; ii) DIAD, triphenylphosphine, toluene, 25 °C, 12 h; iii) K_2CO_3, ethanol, 25 °C, 12 h; iv) KOH, ethanol, 80 °C, 24 h; v) K_2CO_3, propargyl bromide, DMF, 50 °C, 12 h; vi) *n*-alkyl carboxylic acid, EDC·HCl, DMAP, CH_2Cl_2, 25 °C, 12 h.

biocatalyst.[60,61] Dimethyl 5-hydroxyisophthalate (**3**) was subjected to undergo Mitsunobu reaction with 1,3-diacetoxyglycerol (**2**) to yield dimethyl 5-((1,3-diacetoxypropan-2-yl)oxy) isophthalate (**4**). The observance of a peak at 1720 cm^{-1} in the IR spectrum confirms the presence of ester carbonyls in the molecule. The appearance of two singlets (six protons each) at δ 2.07 and 3.94 ppm, accounting for two acetoxy and two methyl ester protons supports the formation of product. The peaks for other protons and carbons were also observed ascertaining the formation of product. Furthermore, the coupling reaction resulted in a downfield shift of the methine protons of the glyceryl moiety from δ 4.05–4.03 ppm[60] to δ 4.80–4.75 ppm and from δ 67.78 ppm to δ 74.52 ppm in the ^{1}H and ^{13}C NMR spectra, respectively. Subsequently compound **4** was subjected to deacetylation in the presence of potassium carbonate followed by methyl ester hydrolysis using KOH to afford 5-((1,3-dihydroxypropan-2-yl)oxy)isophthalic acid (**6**). The disappearance of the two singlets at δ 2.07 and 3.94 ppm in the ^{1}H NMR spectrum along with the appearance of peaks at 3464 and 3319 cm^{-1} corresponding to COOH and OH in the IR spectrum confirmed the complete deprotection in compound **4**. The propargylation of the resulting compound (**6**) yielded the desired A_2B_2 core (**7**), its structure was established by the observance of a triplet (2H) and doublet (4H) at δ 2.53 and 4.93 ppm, respectively in the ^{1}H NMR spectrum. Compound **7** was then subjected to coupling with dodecanoic/pentadecanoic acid using EDC·HCl and DMAP. The compounds **8** and **9** so obtained were completely characterized by their IR, ^{1}H, ^{13}C NMR and HRMS spectra. The presence of hydrophobic chain was ascertained by the appearance of a triplet at 0.81 ppm (J = 6.7 Hz) integrating for six protons and other methylene protons in 1.17–1.24 ppm range in ^{1}H NMR spectrum. mPEG was used to confer hydrophilicity, mPEG-azides (**14** and **15**) were first synthesized from commercially available mPEG-550 (**10**) and mPEG-1000 (**11**) by following the literature report,[62] that is, they were first reacted with methanesulfonyl chloride to get the corresponding mesyl derivatives **12** and **13**, respectively. The mesylated product was then subjected to azidation using sodium azide in DMF. The disappearance of the broad peak of OH group at 3319 cm^{-1} and the appearance of one sharp peak for azide at 2100 cm^{-1} in the IR spectrum confirmed the completion of azidation reaction (Scheme 2).

Finally, four different amphiphiles were synthesized by using the click chemistry approach, that is, The dipropargylated hydrophobic intermediate (**8**/**9**) and hydrophilic mPEG-azide moiety (**14**/**15**) were coupled together using tris (triphenylphosphine) copper(I) bromide and DIPEA in the presence of DMF to yield the desired nonionic gemini amphiphiles **16**–**19** (Scheme 3).

The formation of amphiphiles **16**–**19** was confirmed by the disappearance of azide peak at around 2100 cm^{-1} in the IR spectrum. The formation of the coupled product, for example compound **16**, was further ascertained by the appearance of aromatic protons of triazole moieties at around δ 7.86 ppm in the ^{1}H NMR spectrum. The observance of peaks in the aromatic region corresponding to triazolyl ring carbons at around δ 125 and 142 ppm in the ^{13}C NMR spectrum further support the formation of the desired product. Furthermore, triazole ring formation also results in the observance of characteristic downfield shift for the methylene protons of propargyl moiety from δ 4.93 ppm to 5.43 ppm in the ^{1}H NMR spectrum.

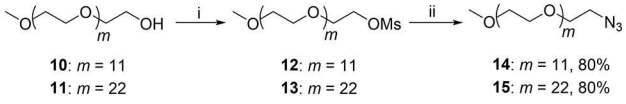

Scheme 2. Synthesis of hydrophilic moieties, mPEG-azide. i) mesyl chloride, triethyl amine, CH_2Cl_2, 0–25 °C, 2 h; ii) sodium azide, DMF, 80 °C, 12 h.

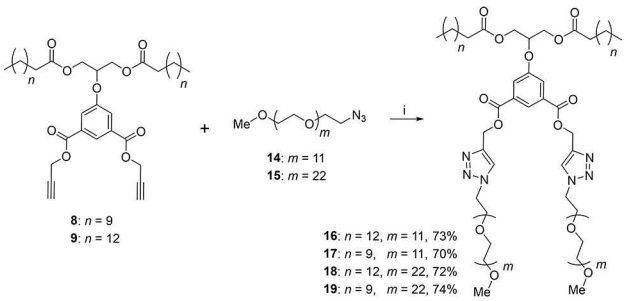

Scheme 3. Synthesis of nonionic gemini amphiphiles. i) [Cu (PPh_3)$_3$]Br, DIPEA, DMF, 60 °C, 24 h.

Physicochemical characterization of amphiphiles and self-assembly study in aqueous medium

DLS, cryo-TEM, HRTEM, UV/Vis and fluorescence spectroscopy were used to study the physicochemical, transport and stimuli-responsive behavior of the mPEG based amphiphiles. GPC was used to determine the molecular weight and polydispersity index (PDI) of the synthesized gemini amphiphiles. The aqueous solution of these amphiphilic architectures displays supramolecular aggregation behavior leading to the formation of nanostructures which were characterized by CAC using Nile Red as a fluorescent probe,[63] and DLS measurement was used for determining the particle size and also the *cryo*-TEM and HRTEM image were recorded to study the morphology of amphiphilic architectures.

Calculation of critical aggregation concentration using fluorescence measurements

The minimum concentration at which the synthesized amphiphiles (**16**–**19**) begin to form the aggregates was determined by using poorly water-soluble dye, Nile Red, as a fluorescent probe.[63] A fixed amount of the dye was used for encapsulation in different concentration of amphiphiles. In the absence of supramolecular aggregates, that is at concentrations below the CAC, the fluorescence intensity of the dye remains low, while gradually increasing the amphiphile concentration, it was observed that at a specific concentration, a considerable increment in the fluorescent intensity occurs because of the surrounding of the dye within the hydrophobic core of the self-assembled nanostructures. A break in the plot of encapsulated dye's fluorescence intensity versus log[amphiphile] gives the CAC value. The CAC of the amphiphilic system **16**–**19** evaluated by fluorescence spectrophotometer was found to be of the order of 10^{-4} to 10^{-5} M (Figure 2 and Table 1), and for the comparison purpose the CAC value of a representative amphiphile **18** was also evaluated by plotting the its conductivity versus its concentration, and the obtained value (2.50×10^{-4}) shows a good correlation with the data from fluorescence spectroscopy (Figure S16b). The hydrophilic-lipophilic balance (HLB) of amphiphiles was calculated by Griffin's equation; that is, $HLB = 20\times M_h/M_w$, where M_w is molecular weight of amphiphiles determined by GPC, and M_h is molecular weight of hydrophilic part.[64] The CAC and the HLB values of all the nanocarriers are shown in Table 1.

Table 1. Physicochemical properties of amphiphiles **16**–**19**.

Amphiphile	DLS size (*d*) [nm]	CAC [M]	HLB
C-15/mPEG-550 (**16**)	12.05	7.84×10^{-5}	11.13
C-12/mPEG-550 (**17**)	10.31	7.70×10^{-5}	11.64
C-15/mPEG-1000 (**18**)	13.70	1.06×10^{-4}	13.69
C-12/mPEG-1000 (**19**)	13.36	9.33×10^{-5}	14.10

Dynamic light scattering and HRTEM measurements

The DLS measurement at a concentration of 5 mg/mL was used to obtain the particle size of the resulting amphiphiles (Table 1). A mostly bimodal size distribution profile in intensity, referring to micelles and micellar aggregates, whereas monomodal in volume and number corresponding to micelles was observed

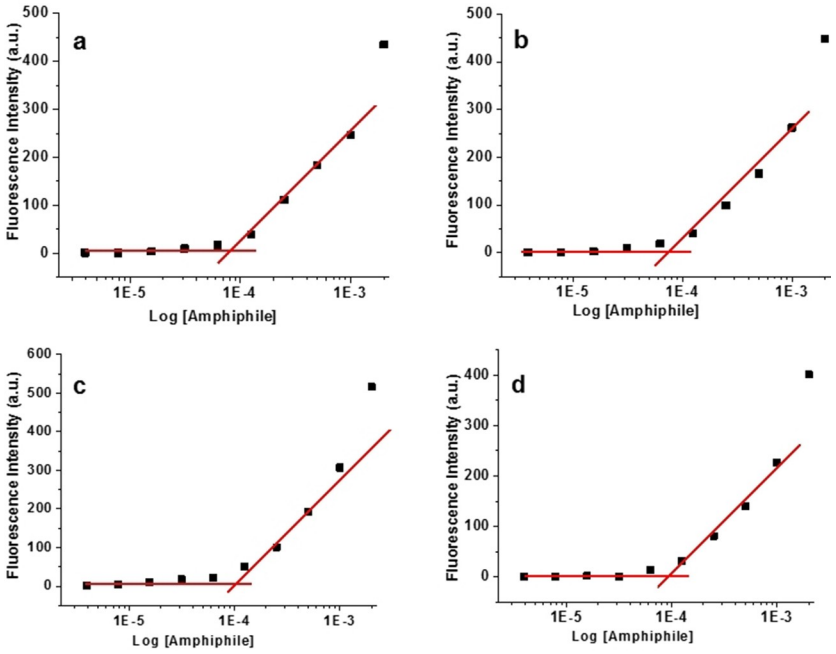

Figure 2. Plots of fluorescence intensity versus log of the concentration of amphiphiles a) **16**, b) **17**, c) **18**, and d) **19** in aqueous solution at 25 °C.

(Figure 3), which suggested that there was a small proportion of micellar aggregates and micelles were the predominant species in aqueous solutions. On comparing the intensity distribution of amphiphiles with mPEG-550/1000 chains in corresponding ratios, the amphiphile with mPEG-1000 hydrophilic chain were observed to be larger than the corresponding analogues containing mPEG-550. Corresponding volume distribution plots display values in the range of 11–13 nm for amphiphiles **16**–**19**. In order to know the actual morphology of the nanostructured architectures formed within the aqueous solution of dendritic mPEG based amphiphiles, *cryo*-TEM micrograph of the aggregates formed from amphiphile **17** shows the formation of small micelles as well as micellar aggregates with a uniform diameter of 7 nm (Figure S15). The study was extended further by recording the HRTEM micrographs of amphiphiles **16**–**19** at a concentration of 5 mg/mL. The HRTEM data uncovered the formation of small micelles as well as micellar aggregates with a uniform diameter of 7–10 nm, which is in good agreement with the corresponding DLS profile as shown in Figure 4.

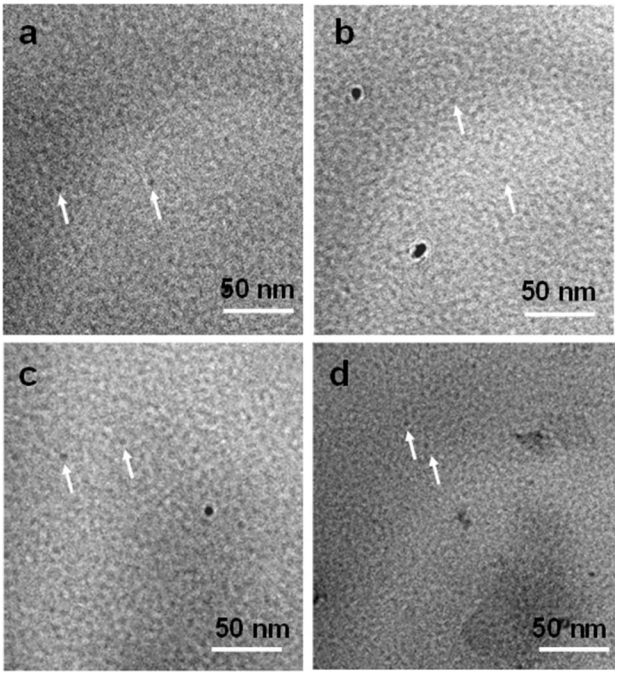

Figure 4. HRTEM micrographs of amphiphiles a) **16**, b) **17**, c) **18** and d) **19** showing small uniform micelles of a diameter 7–10 nm. Scale bars: 50 nm.

Transport potential of amphiphiles for Nile Red and Nimodipine

The applicability of the synthesized nonionic gemini amphiphiles as nanocarriers for hydrophobic guests was investigated using the fluorescent dye, Nile Red and the calcium channel blocker drug, Nimodipine, both of them interact with the nanocarriers through non-covalent interactions such as hydrophobic, π-π stacking and hydrogen bonding. The encapsulation of the compounds was carried by the thin film method.[65] The resulting data of the transport efficiency, transport capacity and encapsulation efficiency are shown in Table 2.

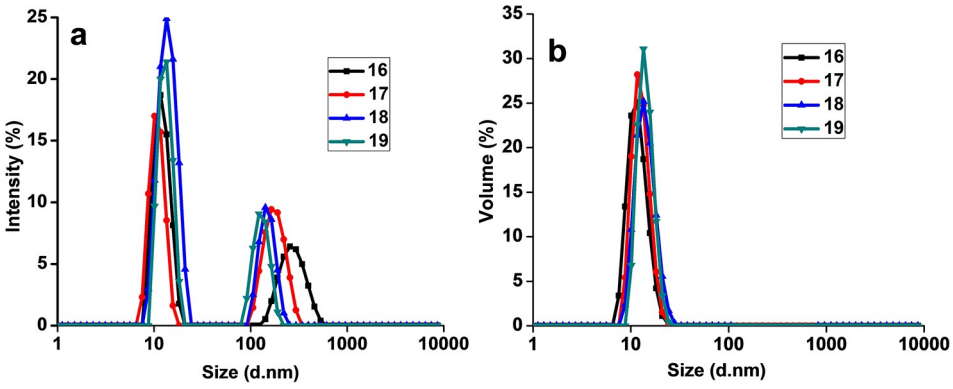

Figure 3. DLS profiles for the amphiphiles **16**–**19** in water. a) intensity graph; b) volume graph.

Table 2. Transport efficiency, transport capacity and encapsulation efficiency of amphiphiles **16**–**19** for Nile Red and Nimodipine

Amphiphile	Transport efficiency [mg/g]		Transport capacity [mmo/mol]		Encapsulation efficiency [%]	
	Nile Red	Nimodipine	Nile Red	Nimodipine	Nile Red	Nimodipine
16	1.13	24.10	6.95	112.50	2.83	7.53
17	1.76	23.68	10.03	105.00	4.42	7.37
18	1.16	20.66	10.69	144.44	2.90	6.45
19	0.64	17.40	5.73	118.18	1.61	5.43

Nile Red encapsulation

Nile Red is a neutral and environmentally sensitive fluorescent dye with limited aqueous solubility. It exhibits highly solvatochromic fluorescence with strong emission in a lipophilic environment. It is very commonly used to predict the position of encapsulated guest and for evaluating the transport potential of nanocarriers.[65] Nile Red is known to form *H*- and *J*-type aggregates, beyond a certain concentration which shows a shoulder additional peak in the absorption spectra.[66] To avoid aggregate formation, we have taken 0.12 mg of the dye with 5 mg/mL of the nanocarrier solution, which is already standardized earlier by our group.[52] For quantification of the amount of Nile Red in various encapsulated samples, the samples were first lyophilized and re-dissolved in a known quantity of methanol for recording their UV/Vis absorbance and fluorescence emission spectra. The transport efficiency and transport capacity of the encapsulated dye or concentration of Nile Red in methanol were then calculated by applying the Beer–Lambert law and using the molar extinction coefficient (ε) of 45 000 $M^{-1}cm^{-1}$ at 552 nm.[52,67] The amphiphile **17** constituted from mPEG-550 and C_{12} alkyl chain exhibit the maximum encapsulation followed by amphiphiles **16**, **18** and **19** (Figure 5).

Nimodipine encapsulation

Nimodipine, a 1,4-dihydropyridine derivative is a well-known calcium channel blocker. It is used to increase the cerebral blood flow in humans as well as in animals.[68] Hydrophobic character of Nimodipine limits its aqueous solubility (0.4 mg/L). For 50 mg of Nimodipine, PEG (62.5 g) and ethanol (37.5 g) are currently used to yield the commercial formulation.[69] In this regard, we synthesized PEG based amphiphilic architectures that enhance the solubility of Nimodipine besides facilitating its encapsulation and circulation in the biological systems. The quantification of Nimodipine per gram of amphiphile was measured using UV/Vis spectrophotometer following the Beer–Lambert law and extinction coefficient of the drug as 7200 $M^{-1}cm^{-1}$ at 365 nm in ethanol. 2.5 g of synthesized amphiphile is required to formulate 50 mg of Nimodipine. Amphiphile **17** consisting of mPEG-550 and C_{12} alkyl chain shows highest encapsulation efficiency and highest transport capacity (Figure 5), it was observed that increasing the size of the mPEG head group from M_n 550 (in **16**, **17**) to 1000 (in **18**, **19**) leads to a considerable decrease in transport capacity for either of the guest molecules. However, increasing the length of the alkyl chain from C_{12} to C_{15} like in the case of amphiphile **16** led to an enhancement of the transport capacity (Figure 5 and Table 2). Qualitative analysis of the data shows that the transport capacity depends on the size of both alkyl and mPEG chains and hydrophobic-lipophilic balance of the amphiphiles.

Nimodipine consists of a 3-nitrophenyl moiety attached to the dihydropyridine unit, a specific EDA-π interactions between the drugs' electron-deficient aromatic ring and the isophthalate moiety of the amphiphile (**16**–**19**) may be the origin for the transport capacity,[70] besides the common hydrophobic interactions (Figure 5). This fact is strengthened further by the observance of stronger absorption peak in the UV–visible spectrum of the solution of nimodipine encapsulated amphiphile (**16**–**19**) in comparison to blank amphiphile (Figure S17). The transportation study also revealed that for both nonpolar guest molecules (Nile Red and Nimodipine) the amphiphile **17** exhibits higher transport potential (Table 2). The solutions of drug encapsulated amphiphiles prepared by simple stirring showed long-term stability up to 115 h at 37 °C that shown by fluorescence spectrometry in Figure 8d, below.

Cell viability study

Good cellular viability is one of the desirable criteria for the synthesis of efficient nanocarriers for biomedical applications. Therefore, the effect of the synthesized amphiphiles (**16**–**19**) on the viability of A549 lung cancer cells was assessed using the CCK-8 Kit after amphiphilic treatment for 24 h using three different test concentrations: 2.0, 1.0 and 0.5 mg/mL (Figure 6). For all tested systems a concentration dependent effect is seen as the cell viability decreases at higher concentration. However, for the amphiphiles **16**, **17** and **19**, the cell's viability is above 80% up to a concentration of 1 mg/mL. On further increasing

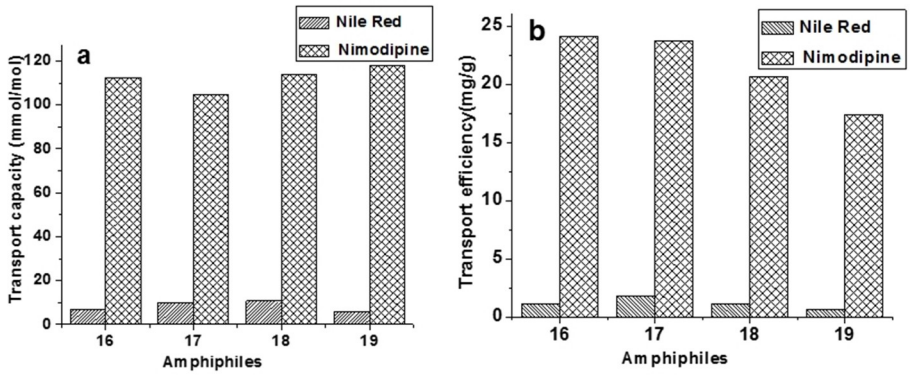

Figure 5. a) Transport capacity and b) transport efficiency of amphiphiles **16**–**19** for Nile Red and Nimodipine.

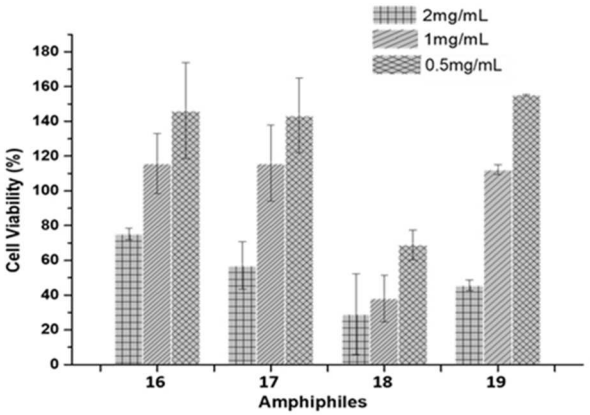

Figure 6. Effect of amphiphiles **16**–**19** on cell viability after 24 h. The viability of the cells treated with the nanocarriers was determined in a CCK-8 assay on A549 cells. Each bar represents the mean value of three independent experiments ($n = 3$) with the standard deviation.

the concentration to 2 mg/mL the cell viability of all of these amphiphiles (**16**, **17** and **19**) reduce to values below 80%. Amphiphile **18** on the other hand is not so well tolerated and even at a concentration of 0.5 mg/mL the cell viability is less than 80%. Interestingly, amphiphiles **16**, **17** and **18** show promotion of cell growth most probably due to better cell adhesion that could influence the cytotoxicity of the carrier systems. In summary it can be concluded that the amphiphiles constructed from a C_{15}/C_{12} alkyl chain with mPEG-550, that is, **16** and **17**, are better tolerated than the analogues **18** and **19** having mPEG-1000 moiety. In cell viability test, all of the amphiphiles were found to be safe for 24 h at each tested concentration. Similar types of amphiphiles were earlier measured for cytotoxic studies by our group,[49] but no significant difference was observed on cell viability on going from 24 to 72 h, thus we confined the study for 24 h at different concentrations.

Cellular uptake study

Amphiphiles **16** and **17** exhibit the highest encapsulation for Nile Red, therefore, the cellular uptake potential of Nile Red encapsulated in these two amphiphiles was studied by confocal laser scanning microscopy (CLSM) using A549 lung cancer cells. The Nile Red encapsulated supramolecular architectures were prepared by incubating the dye in an aqueous solution of amphiphile using the film method at a concentration of 5 mg/mL. The CLSM image (Figures 7 and S14) reveal that the dye encapsulated in amphiphiles **16** and **17** can be internalized into cells and after 4 h, a strong signal is seen inside the cell's cytosol (Figure S14). After 24 h, the fluorescence intensity of the Nile Red inside the cells increased, indicating a continuous uptake of the encapsulated dye and accumulating over time. In order to establish a proof-of-concept to use these amphiphiles as nanocarriers, their general tolerability in cells was studied by using A549 cell lines.[49,71]

Enzyme triggered release study

In order to develop an efficient drug delivery system, the release of encapsulated therapeutic from the nanocarrier in a controlled manner is very essential. As the amphiphiles reported herein are constituted from ester linkages that might offer sensitivity to pH/enzyme mediated hydrolytic conditions, we decided to explore the ester hydrolysis of amphiphiles using immobilized *C. antarctica* lipase (Novozym 435). Our group has reported earlier the selective hydrolysis of aliphatic acid ester group over the aromatic acid ester in the presence of Novozym

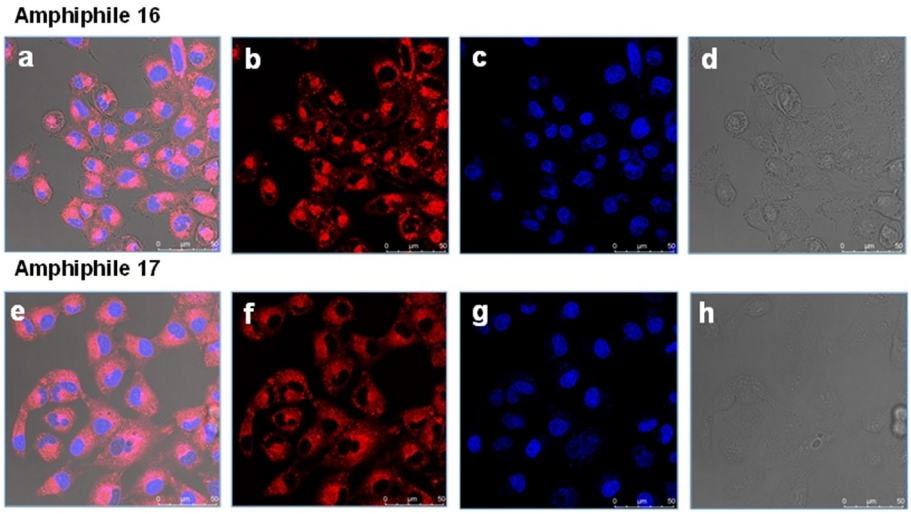

Figure 7. Images taken by confocal laser scanning fluorescence microscopy images from A549 cells after 24 h of incubation with Nile Red encapsulated in amphiphiles **16** (top) and **17** (bottom). In the images, fluorescence from the Nile Red dye is shown in red colour, the fluorescence of DNA stained with Hoechst 33342 indicating the cell nucleus is shown in blue colour, and transmitted light images are in greyscale. Scale bar: 50 μm.

435.[72] Subjecting the synthesized nanoaggregates under such hydrolytic conditions it is anticipated that the nanoarchitecture will eventually start collapsing and the encapsulated hydrophobic guest will be released in a controlled manner. We investigated the time dependent release of encapsulated Nile Red from the core shell of nanocarriers by means of fluorescence spectroscopy. To the solution of dye encapsulated in the amphiphile was added 200 wt% of Novozym 435 and a few drops of *n*-butanol for trapping the acid liberated from ester hydrolysis of the amphiphile.[73] The solution was incubated at 37 °C under dark conditions and the progress of dye release was monitored by drawing aliquots of reaction mixture at regular intervals and measuring their fluorescence spectrum, Figure 8a and b represent the time-dependent decay of fluorescence intensity of Nile Red loaded in amphiphile **17** under physiological conditions in the absence, and presence of the enzyme, respectively. Approximately 50% decay in the intensity occurred after 72 h and it was possible to have more than 90% dye release only after 115 h (Figure 8b). In Table 2, 4.42% Nile Red encapsulate in amphiphile (**17**). The encapsulated Nile Red was found to release within 115 h, interestingly, the dye encapsulated nanocarrier under physiological conditions in the absence of the enzyme was observed to be stable; in fact, insignificant amount of Nile Red was released from the system adopting such conditions.

Conclusion

Herein, we have reported a "greener" chemoenzymatic method to synthesize nonionic gemini amphiphiles from easily available and biocompatible starting materials by incorporating different alkyl chains and mPEGs on a newer type of A_2B_2 core synthesized by conjugation of glycerol and propargyl bromide on 5-hydroxy isophthalic acid in a multiple step chemoenzymatic approach. All of the synthesized amphiphiles were well characterized from their spectroscopic and physical data, for example, ^{1}H NMR, ^{13}C NMR, HRMS, Elemental analysis and GPC techniques. The amphiphilic systems have the tendency to form nano-sized aggregates in aqueous medium with CAC in the range of 10^{-4} – 10^{-5} M and micellar size in the range of 10–14 nm. Cryo-TEM and HRTEM data of the amphiphiles further support the morphology of amphiphiles. The nanotransport potential of amphiphiles was investigated using model hydrophobic guests, that is, the fluorescent dye Nile Red and drug Nimodipine. The results show that the dye was more efficiently

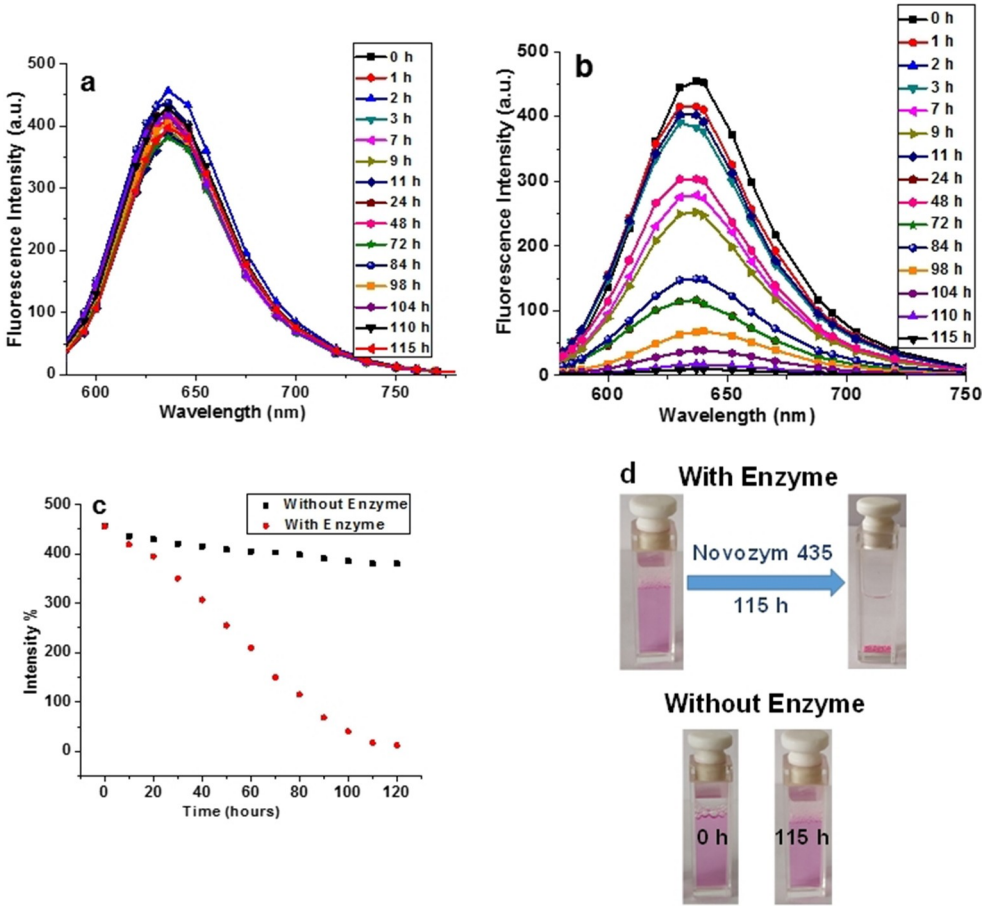

Figure 8. Release profile of Nile Red encapsulated in nanocarrier **17** under physiological conditions. Variation of fluorescence intensity with time of amphiphile-encapsulated Nile Red in the a) absence and b) presence of enzyme at 37 °C. c) Comparison of fluorescence intensity variation of the dye with time in the presence (red) and absence (black) of enzyme at 37 °C. d) Time-dependent release of Nile Red from amphiphile with/without enzyme after 115 h.

encapsulated by amphiphiles having a lower HLB value when compared with Nimodipine. Efficient uptake of encapsulated dye in the cytosol of lung cancer cells was shown by confocal microscopy indicating that the amphiphilic systems can transport drugs into cells. The performed cell viability study showed that the synthesized amphiphiles are relevant as a drug delivery system. The enzyme triggered release profile of the encapsulated dye revealed that approximately 50% decay in the fluorescence intensity occurred after 72 h in the presence of the enzyme with more than 90% release taking place in 115 h.

Experimental Section

IR, NMR spectroscopy, HRMS and GPC analysis

Infrared spectra (IR) of neat samples were recorded using a PerkinElmer FTIR model 9 spectrometer. The ^{1}H and ^{13}C NMR spectra were recorded on JEOL 400 MHz spectrometer. The ^{1}H NMR spectra were calibrated using the residual solvent peak, where the chemical shift values are on a δ scale and the coupling constant (J) values are in Hertz. High-resolution mass spectrometry (HRMS) data were recorded on Q-TOF LCMS-Agilent Technology-6530 and HPLC/MS-Agilent 6210 (Agilent Technologies). A Water's GPC system equipped with a Waters 515 HPLC pump and refractive index (RI) detector was used to determine the molecular weight M_w, M_n and polydispersity index (PDI) of the amphiphiles using Styragel HR column with THF as an eluent at a flow rate of 1.2 mL min^{-1} and polystyrene standards were used for molecular weight calibration.

Acknowledgements

We gratefully acknowledge the Department of Science and Technology (DST), Government of India and DFG, Germany for financial support and University of Delhi to partially support the research under Faculty Research Program (FRP-2020-21) and also thankful to the CRF IIT Delhi for providing assistance in the analysis of the samples. The helpful suggestions of Dr. Abhishek K. Singh are gratefully acknowledged.

Conflict of Interest

The authors declare no conflict of interest.

Keywords: amphiphiles · cellular uptake · controlled release · drug delivery · nanostructures · self-assembly

[1] J. A. A. W. Elemans, A. E. Rowan, R. J. M. Nolte, *J. Mater. Chem.* **2003**, *13*, 2661–2670.
[2] F. J. M. Hoeben, P. Jonkheijm, E. W. Meijer, A. P. H. J. Schenning, *Chem. Rev.* **2005**, *105*, 1491–1546.
[3] S. Prasad, K. Achazi, C. Böttcher, R. Haag, S. K. Sharma, *RSC Adv.* **2017**, *7*, 22121–22132.
[4] R. C. Claussen, B. M. Rabatic, S. I. Stupp, *J. Am. Chem. Soc.* **2003**, *125*, 12680–12681.
[5] J. P. Hill, W. Jin, A. Kosaka, T. Fukushima, H. Ichihara, T. Shimomura, K. Ito, T. Hashizume, N. Ishii, T. Aida, *Science* **2004**, *304*, 1481–1483.
[6] P. K. Vemula, G. John, *Acc. Chem. Res.* **2008**, *41*, 769–782.
[7] A. V. Kabanov, V. A. Kabanov, *Adv. Drug Delivery Rev.* **1998**, *30*, 49–60.
[8] A. Rosler, G. W. M. Vandermeulen, H.-A. Klok, *Adv. Drug Delivery Rev.* **2001**, *53*, 95–108.
[9] D. M. Vriezema, M. C. Aragonès, J. A. A. W. Elemans, J. J. L. M. Cornelissen, A. E. Rowan, R. J. M. Nolte, *Chem. Rev.* **2005**, *105*, 1445–1489.
[10] Y. Wang, H. Xu, N. Ma, Z. Wang, X. Zhang, J. Liu, J. Shen, *Langmuir* **2006**, *22*, 5552–5555.
[11] M. Häger, F. Currie, K. Holmberg, *Top. Curr. Chem.* **2003**, *227*, 53–74.
[12] M. Morikawa, M. Yoshihara, T. Endo, N. Kimizuka, *Chem. Eur. J.* **2005**, *11*, 1574–1578.
[13] S. I. Stupp, L. C. Palmer, *Chem. Mater.* **2014**, *26*, 507–518.
[14] Y. Wang, H. Xu, X. Zhang, *Adv. Mater.* **2009**, *21*, 2849–2864.
[15] Y.-b. Lim, K.-S. Moon, M. Lee, *Chem. Soc. Rev.* **2009**, *38*, 925–934.
[16] J. N. Isrealachvili, D. J. Mitchell, B. W. Ninham, *J. Chem. Soc. Faraday Trans. 2*, **1976**, *72*, 1525–1568.
[17] J. N. Israelachvili, *Intermolecular and Surface Forces*, Academic Press, New York, **1985**.
[18] H. V. Berlepsch, K. Ludwig, B. Schade, R. Haag, C. Böttcher, *Adv. Colloid Interface Sci.* **2014**, *208*, 279–292.
[19] H.-J. Kim, T. Kim, M. Lee, *Acc. Chem. Res.* **2011**, *44*, 72–82.
[20] K. G. Goswami, S. Mete, S. S. Chaudhury, P. Sar, E. Ksendzov, C. D. Mukhopadhyay, S. V. Kostjuk, P. De, *ACS Appl. Polym. Mater.* **2020**, *2*, 2035–2045.
[21] M. Mammen, S.-K. Choi, G. M. Whitesides, *Angew. Chem. Int. Ed.* **1998**, *37*, 2754–2794; *Angew. Chem.* **1998**, *110*, 2908–2953.
[22] A. Mulder, J. Huskens, D. N. Reinhoudt, *Org. Biomol. Chem.* **2004**, *2*, 3409–3424.
[23] S. Gupta, R. Tyagi, V. S. Parmar, S. K. Sharma, R. Haag, *Polymer* **2012**, *53*, 3053–3078.
[24] A. J. ten Tije, J. Verweji, W. J. Loos, A. Sparreboom, *Clin. Pharmacokinet.* **2003**, *42*, 665–833.
[25] C. Wang, Z. Wang, X. Zhang, *Small* **2011**, *7*, 1379–1383.
[26] S. Pal, S. G. Roy, P. De, *Polym. Chem.* **2014**, *5*, 1275–1284.
[27] C. Wang, Z. Wang, X. Zhang, *Acc. Chem. Res.* **2012**, *45*, 608–618.
[28] A. Sorrenti, O. Illa, R. M. Ortuño, *Chem. Soc. Rev.* **2013**, *42*, 8200–8219.
[29] T. Shimizu, M. Masuda, H. Minamikawa, *Chem. Rev.* **2005**, *105*, 1401–1443.
[30] L. C. Palmer, S. I. Stupp, *Acc. Chem. Res.* **2008**, *41*, 1674–1684.
[31] N. Singh, L. Sharma, *Lett. Org. Chem.* **2019**, *16*, 607–614.
[32] R. S. G. Krishnan, S. Thennarasu, A. B. Mandal, *J. Phys. Chem. B* **2004**, *108*, 8806–8816.
[33] B. Trappmann, K. Ludwig, M. R. Radowski, A. Shukla, A. Mohr, H. Rehage, C. Böttcher, R. Haag, *J. Am. Chem. Soc.* **2010**, *132*, 11119–11124.
[34] F. Bordi, G. Cerichelli, N. D. Berardinis, M. Diociaiuti, L. Giansanti, G. Mancini, S. Sennato, *Langmuir* **2010**, *26*, 6177–6183.
[35] L. Shi, F. Chen, N. Sun, L. Zheng, *Soft Matter* **2015**, *11*, 4075–4080.
[36] G. Paddon-Jones, S. Regismond, K. Kwetkat, R. Zana, *J. Colloid Interface Sci.* **2001**, *243*, 496–502.
[37] A. R. Tehrani-Bagha, R. G. Singh, K. Holmberg, *J. Colloid Interface Sci.* **2012**, *376*, 112–118.
[38] M. Dreja, W. Pyckhout-Hintzen, H. Mays, B. Tieke, *Langmuir* **1999**, *15*, 391–399.
[39] W. Zhao, Y. Wang, *Adv. Colloid Interface Sci.* **2017**, *239*, 199–212.
[40] R. Zana, *Adv. Colloid Interface Sci.* **2002**, 97, 205–253.
[41] Y. Han, Y. Wang, *Phys. Chem. Chem. Phys.* **2011**, *13*, 1939–1956.
[42] L. D. Song, M. J. Rosen, *Langmuir* **1996**, *12*, 1149–1153.
[43] H. Lv, S. Zhang, B. Wang, S. Cui, J. Yan, *J. Controlled Release* **2006**, *114*, 100–109.
[44] M. A. Rub, A. M. Asiri, A. Z. Naqvi, M. M. Rahman, S. B. Khan, K. -ud-Din, *J. Mol. Liq.* **2013**, *177*, 19–25.
[45] D. R. Sikwal, R. S. Kalhapure, M. Jadhav, S. Rambharose, C. Mocktar, T. Govender, *RSC Adv.* **2017**, *7*, 14233–14246.
[46] S. Liu, R. Sang, S. Hong, Y. Cai, H. Wang, *Langmuir* **2013**, *29*, 8511–8516.
[47] M. J. L. Castro, J. Kovensky, A. F. Cirelli, *Langmuir* **2002**, *18*, 2477–2482.
[48] B. Parshad, P. Yadav, Y. Kerkhoff, A. Mittal, K. Achazi, R. Haag, S. K. Sharma, *New J. Chem.* **2019**, *43*, 11984–11993.
[49] A. K. Singh, B. N. S. Thota, B. Schade, A. Khan, C. Böttcher, S. K. Sharma, R. Haag, *Chem. Asian J.* **2017**, *12*, 1796–1806.
[50] A. Mittal, A. K. Singh, A. Kumar, Parmanand, K. Achazi, R. Haag, S. K. Sharma, *Polym. Adv. Technol.* **2020**, *31*, 1208–1217.
[51] Parmanand, A. Mittal, A. K. Singh, Aarti, K. Achazi, C. Nie, R. Haag, S. K. Sharma, *RSC Adv.* **2020**, *10*, 37555–37563.
[52] M. Kumari, S. Gupta, K. Achazi, C. Böttcher, J. Khandare, S. K. Sharma, R. Haag, *Macromol. Rapid Commun.* **2014**, *36*, 254–261.

[53] J. M. Harris, *Topics in Applied Chemistry*: Poly(ethylene glycol) Chemistry: Biotechnical and Biomedical Applications, Plenum, New York, **1992**.
[54] N. Sadhukhan, T. Muraoka, D. Abe, Y. Sasanuma, D. R. G. Subekti, K. Kinbara, *Chem. Lett.* **2014**, *43*, 1055–1057.
[55] K. Knop, R. Hoogenboom, D. Fischer, U. S. Schubert, *Angew. Chem. Int. Ed.* **2010**, *49*, 6288–6308; *Angew. Chem.* **2010**, *122*, 6430–6452.
[56] S. Zalipsky, *Adv. Drug Delivery Rev.* **1995**, *16*, 157–182.
[57] B. Obermeier, F. Wurm, C. Mangold, H. Frey, *Angew. Chem. Int. Ed.* **2011**, *50*, 7988–7997; *Angew. Chem.* **2011**, *123*, 8136–8146.
[58] R. Kumar, M.-H. Chen, V. S. Parmar, L. A. Samuelson, J. Kumar, R. Nicolosi, S. Yoganathan, A. C. Watterson, *J. Am. Chem. Soc.* **2004**, *126*, 10640–10644.
[59] H. Donga, L. Panga, H. Conga, Y. Shena, B. Yua, *Drug Delivery* **2019**, *26*, 416–432.
[60] S. Gupta, B. Schade, S. Kumar, C. Böttcher, S. K. Sharma, R. Haag, *Small* **2013**, *9*, 894–904.
[61] A. Halldorsson, C. D. Magnusson, G. G. Haraldsson, *Tetrahedron* **2003**, *59*, 9101–9109.
[62] M. B. van Eldijk, F. C. M. Smits, N. Vermue, M. F. Debets, S. Schoffelen, J. C. M. van Hest, *Biomacromolecules* **2014**, *15*, 2751–2759.
[63] A. Klaikherd, C. Nagamani, S. Thayumanavan, *J. Am. Chem. Soc.* **2009**, *131*, 4830–4838.
[64] W. C. Griffin, *J. Soc. Cosmet. Chem.* **1949**, *1*, 311–326.
[65] E. Fleige, B. Ziem, M. Grabolle, R. Haag, U. Resch-Genger, *Macromolecules* **2012**, *45*, 9452–9459.
[66] I. N. Kurniasih, H. Liang, S. Kumar, A. Mohr, S. K. Sharma, J. P. Rabe, R. Haag, *J. Mater. Chem. B* **2013**, *1*, 3569–3577.
[67] R. P. Haugland, *Handbook of Fluorescent Probes and Research Chemicals*, 6th ed., Molecular Probes. Eugene, **1996**.
[68] D. Tomassoni, A. Lanari, G. Silvestrelli, E. Traini, F. Amenta, *Clin. Exp. Hypertens.* **2008**, *30*, 744–766.
[69] H. Türk, A. Shukla, P. C. A. Rodrigues, H. Rehage, R. Haag, *Chem. Eur. J.* **2007**, *13*, 4187–4196.
[70] S. K. Sharma, R. Kumar, S. Kumar, R. Mosurkal, V. S. Parmar, L. A. Samuelson, A. C. Watterson, J. Kumar, *Chem. Commun.* **2004**, *23*, 2689–2691.
[71] Rashmi, A. K. Singh, K. Achazi, S. Ehrmann, C. Böttcher, R. Haag, S. K. Sharma, *Polym. Chem.* **2020**, *11*, 6772–6782.
[72] A. K. Singh, R. Nguyen, N. Galy, R. Haag, S. K. Sharma, C. Len, *Molecules* **2016**, *21*, 1038.
[73] B. Norjannah, H. C. Ong, H. H. Masjuki, J. C. Juan, W. T. Chong, *RSC Adv.* **2016**, *6*, 60034–60055.

Manuscript received: January 14, 2021
Revised manuscript received: February 5, 2021
Accepted manuscript online: February 8, 2021
Version of record online: March 8, 2021